Assessment of breast cancer progression and metastasis during a hypercoagulable state induced by silencing of antithrombin in a xenograft mouse model

Buijs, J.T.; Unlu, B.; Laghmani, E.H.; Heestermans, M.; Vlijmen, B.J.M. van; Versteeg, H.H.

Thrombosis Research 221 (2023) 51–57

Contents lists available at ScienceDirect

Thrombosis Research

journal homepage: www.elsevier.com/locate/thromres

Full Length Article

Assessment of breast cancer progression and metastasis during a hypercoagulable state induced by silencing of antithrombin in a xenograft mouse model

J.T. Buijs, B. Ünlü, E.H. Laghmani, M. Heestermans, B.J.M. van Vlijmen, H.H. Versteeg *

Einthoven Laboratory for Vascular and Regenerative Medicine, Division of Thrombosis and Hemostasis, Department of Medicine, Leiden University Medical Centre, Leiden, the Netherlands

ARTICLE INFO

Keywords:
Breast cancer
Metastasis
Antithrombin
Cancer-associated thrombosis
Mouse model

ABSTRACT

Local coagulation activation has been shown to impact both primary tumor growth and metastasis in mice. It is well known that components of the blood clotting cascade such as tissue factor and thrombin play a role in tumor progression by activating cellular receptors and local formation of fibrin. However, whether venous thromboembolism (VTE) or a hypercoagulable state has a direct impact on cancer progression is unknown. Here we have combined an orthotopic murine breast cancer model, using female Nod-SCID mice, with siRNA-mediated silencing of antithrombin (siAT) leading to the induction of a systemic hypercoagulable state. We show that, compared to control siRNA-treated (not experiencing a hypercoagulable state) tumor-bearing mice, siAT treated tumor-bearing mice do not show enhanced tumor growth nor enhanced metastasis. We conclude that, in this murine model for hypercoagulability, induction of a hypercoagulable state does not contribute to breast cancer progression.

1. Introduction

Experimental models have shown that the blood clotting machinery plays an active role in tumor progression [1]. Blood clotting normally starts when blood coagulation protein tissue factor (TF) becomes exposed to the blood stream because of trauma [2]. TF then binds blood borne FVIIa to generate blood clotting factor FXa which subsequently leads to thrombin generation and a fibrin clot. TF has been shown to drive both primary tumor growth as well as metastasis [3,4]. The TF:FVIIa complex plays a role in tumor angiogenesis through activation of tumor cell receptor Protease-activated Receptor (PAR)-2 [5]. In addition, TF:FVIIa mediates local generation of fibrin, protecting metastatic cells from the immune system [6]. Similarly, thrombin also impacts tumor progression by facilitating tumor angiogenesis and metastasis [7]. In line with this, several clinical studies have shown that prophylactic use of anticoagulants may have beneficial effects in cancer patients with a good prognosis [8,9]. In contrast, a meta-analysis performed in 2014 detected no survival benefit of anticoagulants in cancer patients, but this meta-analysis did not look at the effects of anticoagulants in patients with limited-stage disease [10].

Vice versa, cancer patients have an increased risk of venous thromboembolism (VTE; the composite of deep venous thrombosis and pulmonary embolism) resulting from hyperactivation of the blood clotting cascade [11,12]. Nevertheless, at present it is unclear whether VTE also adds to tumor progression. We have recently shown that colorectal cancer patients experiencing VTE have enhanced levels of fibrin in their tumors [13] which could either lead to immune cell infiltration or a cessation of tumoral blood flow leading to hypoxia. Both processes are linked to metastasis, and therefore, VTE could indirectly link to metastasis. In this study, we set out to explore, using tumor bearing mice subjected to acute lowering of Antithrombin (AT), whether presence of a hypercoagulable state leads to enhanced metastasis.

2. Material and methods

2.1. Cells

Previously established MDA-MB-231 breast cancer cells with high propensity to metastasize to lungs – MDA-MB-231-GFP-LC - were used [14], and cultured as described previously [14].

* Corresponding author.
E-mail address: h.h.versteeg@lumc.nl (H.H. Versteeg).

https://doi.org/10.1016/j.thromres.2022.11.018
Received 4 February 2022; Received in revised form 14 October 2022; Accepted 21 November 2022
Available online 25 November 2022

2.2. In vivo experiments

Mice were housed at the central animal facility of the LUMC at biosafety level D1. The FELASA recommendations for the health monitoring in experimental units were used. Mice were housed in Sealsafe® PLUS, green line system (Tecniplast S.p.A.) autoclaved GM500 cages, with autoclaved LIGNOCEL® BK 8–15 (BK-8-15-00433, JRS) bedding material. Daytime was set at 7:00 to 18:00 with sunrise and sunset set at 6:30 to 7:00 and 18:00 to 18:30, respectively. Light intensity was 40 to 80 LUX at top of the racks and 10 to 30 LUX inside the bottom and top cages. Temperature was set at 20 °C to 22 °C, and water was provided ad libitum in autoclaved plastic drinking bottles (Tecniplast S.p.A.) and refreshed weekly. Mice were fed regular chow-diet (RM3 diet, pelleted), ad libitum. Mice were acclimatized for 7 days after arrival before the start of the experiment. To establish breast tumors in mice, orthotopic injections were performed as follows; 1×10^6 MDA-MB-231 cells in a volume of 50 μl PBS were injected into the 4th mammary fatpad of 6 week-old female Nod-SCID mice (Charles River, Wilmington, MA, USA). In the study, only female mice were used as implanted breast cancer cells were implanted orthotopically into the 4th mammary fatpad. In male mice, mammary fatpad are underdeveloped. During surgery, mice were under anaestesia using 2.5 % isoflurane at 2–3 l/min O_2. Temgesic (0.1 mg/kg body weight, s.c. injected; Schering-Plough, Kenilworth, NJ, USA) was used as analgesic. Tumor volume was determined every 3–4 days using a caliper and the formula: (length × width^2) / 2. After each measurement, the 2 cages were placed in alternating order back in the rack. An a priori sample size calculation resulted in a sample size of 4 mice per group using an expected 2-fold difference in metastasis as detected with human specific qPCR, an expected standard deviation of 30 %, a *P*-value of 0.05 and a power of 80 %. To prevent that the potential loss of 1 mouse in the siAT-treated group during the experiment would reduce the power in the study, one mouse was added, totaling 9 mice housed in two cages. Mice were marked by a permanent marker on the tail and all mice retained in their own cage, also after allocating to control or treatment group. When tumors reached a volume of 100 mm^3, mice were randomized using a computer-generated random allocation, into groups; one group receiving intravenous injection of Invivofectamine 3.0 (Invitrogen, Carlsbad, CA, USA)-complexed control siRNA (siNEG) or antithrombin-specific siRNA (siAT) (Ambion, Carlsbad, CA, USA; dose siRNA 1.2 mg siRNA per kg body weight).

Mice were closely inspected for fourteen days after injection, and screened for clinical signs typical of a low AT-induced hypercoagulable state (weight loss and periocular hemorrhages secondary to formation of thrombi in the head). Investigators were not blinded to the treatment. Four, five and six days after injection siRNAs, all mice received a bolus injection of 0.5 ml 5 % glucose, as siAT treated mice were somewhat lethargic, and did not eat and drink well. Citrated blood samples were collected from the tail after tail cutting as described previously [15,16] (with some modifications; only 5 mm of tail was cut each time) for plasma antithrombin analysis and blood cellular composition using the Sysmex XP-300 system (Sysmex Corporation, Kobe, JP) at the time points indicated in the figure legends. After 14 days, mice were sacrificed, tumors, lungs, livers and tibiae were collected and frozen in liquid nitrogen for real-time PCR measurements of metastasis (see below). Mouse heads were collected and fixed in 4 % formaldehyde for histochemical analysis. Humane endpoints for this study included reduced mobility, ruffled fur, reduced food consumption or a loss in weight of >20 %. All animal experiments were approved by the animal welfare committee of the Leiden University Medical Center (#11600).

2.3. ELISA

Plasma antithrombin and fibrinogen protein levels were assessed using a murine ELISA kit (Affinity Biologicals, STAGO, Leiden, The Netherlands) according to manufacturer's protocol. Pooled plasma from mice was set as a reference.

2.4. qPCR

Quantitative PCR (qPCR) was used to quantitate metastatic human tumor cells in distant organs using human specific primers for *GAPDH* (Fwd: 5′-TTCCAGGAGCGAGATCCCT-3′; Rev.: 5′-CACCCATGACGAACATGGG-3′) and mouse-specific primers for *ACTB* (Fwd: 5′-AGGTCATCACTATTGGCAACGA-3′; Rev.: 5′-CCAAGAAGGAAGGCTGGAAAA-3′) as described previously [17].

2.5. Histochemistry

Heads were decalcified in 20 % formic acid, dehydrated, embedded in paraffin, and sectioned. After analysis of coronal serial sections of the head and neck, 5-μm sections were made starting directly caudal of the eyes, because this area was most clearly and reproducibly affected and because thrombi in large veins were found here [18]. Selected sections were stained by using hematoxylin and eosin.

2.6. Western blot

Fibrin deposits in tumors were determined by western blotting as described previously [13]. In brief, fibrin was extracted from tumors, equal protein concentrations were loaded onto a 4–12 % Bis-Tris Plus Gel (Thermo Fisher Scientific, Waltham, MA, USA) for 20 min at 200 V and blotted onto a 0.2 mm pore size polyvinylidene difluoride (PVDF) membrane. Membranes were blocked with 5 % low fat milk powder in Tris buffered saline with Tween-20 (TBST) for 1 h. Blots were incubated with mAb 59D8 (a kind gift from Dr. C. Esmon, Oklahoma City, OK, USA) overnight at 4 °C. After extensive washing in TBST, the membrane was incubated with a horseradish peroxidase-conjugated anti-mouse secondary antibody for 1 h at room temperature. Antigen was visualized with Western Lightning Plus ECL (Perkin-Elmer, Waltham, MA, USA) using the Chemidoc imaging system (Biorad, Veenendaal, Netherlands).

2.7. Statistical analysis

Two-way ANOVA with Bonferroni's post-hoc testing was used to analyze data points collected in time. A Mann Whitney test was used when samples were collected at one point in time. *P*-values <0.05 were considered significant. Graphpad Prism was used to determine statistics including data distribution. Metastatic burden was not normally distributed, justifying use of the Mann Whitney test.

3. Results and discussion

3.1. Induction of a hypercoagulable state in tumor-bearing mice

To investigate if a hypercoagulable state drives metastasis, we first grafted MDA-MB-231 triple negative breast cancer cells in the mammary fat pad of Nod-SCID mice as described before [19]. When the tumors reached an average dimension of 100 mm^3 (21 days after tumor cell graftment), mice were injected with Invivofectamine-complexed control siRNA (siNEG) or siRNA against hepatic antithrombin (siAT) (Fig. S1). Similar antithrombin siRNA approaches in combination with protein C knockdown were previously shown to result in large occlusive thrombi in particular in the large veins of the mandibular area of the head, as well as liver and lung fibrin deposition [18]. Upon injection of tumor-bearing mice with siAT, from 2 days on, we observed a drop in antithrombin levels (Fig. 1A), as expected. Within 7 days, all siAT-treated mice showed the periocular hemorrhages as a clinical manifestation of the thrombosis in the large veins of the head (Fig. 1B) as described before [18] and additionally a considerable but transient weight loss (Fig. 1C). Lack of plasma precluded us from determining other markers of a hypercoagulable state such as d-dimer. Signs of periocular hemorrhages gradually disappeared and body weight returned to normal within 14 days after siRNA injection. At sacrifice, histological analysis of

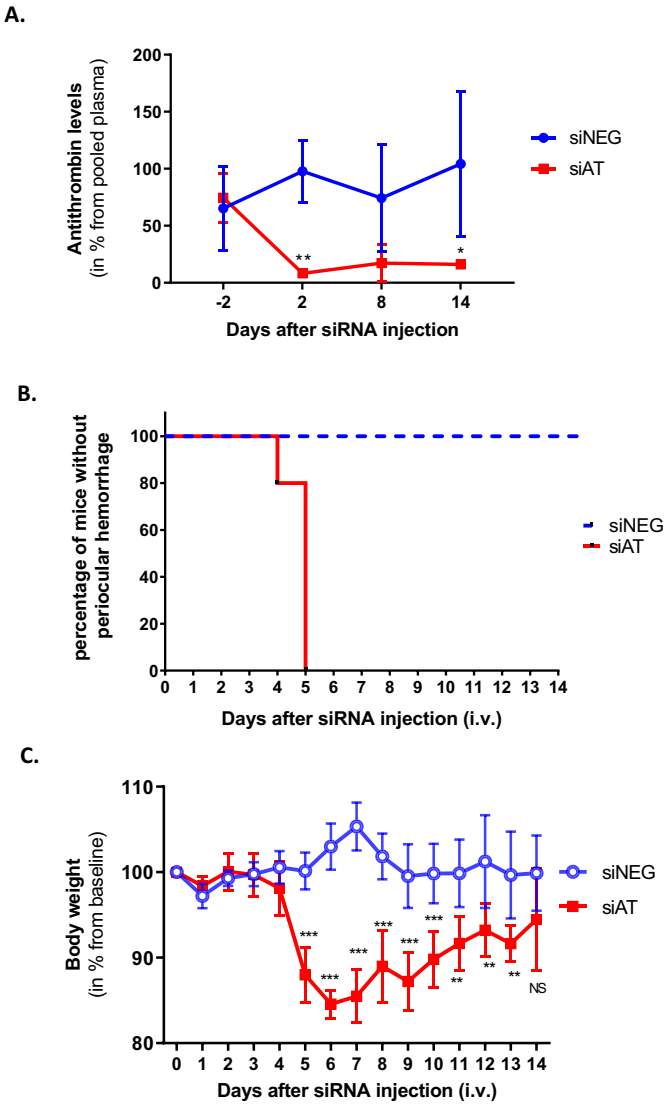

Fig. 1. Effects of systemic knockdown of antithrombin in MDA-MB-231 tumor bearing mice. NOD-SCID mice were injected with invivofectamine-complexed siRNA against antithrombin (siAT) ($n = 5$) or negative control (siNEG) ($n = 4$). A. Plasma antithrombin levels assessed by ELISA confirmed knockdown of antithrombin. After injection of siRNAs, all mice were assessed daily for signs of a hypercoagulable phenotype (exemplified by periocular hemorrhages in this model) (B) and weight loss (C). Data are represented as mean with standard deviation $^{*}P < 0.05$, $^{**}P < 0.01$, $^{***}P < 0.001$ using two-way ANOVA with Bonferroni post-hoc testing.

the mandibular area of the head confirmed the presence of large venous thrombotic lesions essentially as described before [18], as well as fibrin-rich accumulates in major vessels (Fig. S2), confirming the effectiveness of this siAT approach.

We then examined blood parameters such as red blood cell, platelet and white blood cell content. We observed a drop in red blood cells (Fig. 2A), hematocrit (Fig. 2B) and hemoglobin (Fig. 2C) upon siAT treatment, and a slight increase in mean corpuscular volume (Fig. 2D). These findings are consistent with the hemorrhagic phenotype of this hypercoagulable state model. In contrast, we did not observe differences in platelet (Fig. 2E) or white blood cell numbers (Fig. 2G), although mean platelet volume was temporarily increased (Fig. 2F).

3.2. Effects of a hypercoagulable state on tumor progression

Tumor volume in mice receiving siNEG or siAT was recorded every 3–4 days. We did not observe any statistically significant differences in tumor volume (Fig. 3A) or weight at sacrifice (Fig. 3B) between mice receiving siNEG or siAT, ruling out an effect of an siAT-induced hypercoagulable state on primary tumor growth. Biochemical analysis revealed fibrin deposition in tumors of 2 of the 5 siAT-treated mice (Fig. 3C, D).

We then determined metastatic capacity in mice treated with siNEG or siAT, specifically in the lungs, the livers and the bones (tibiae). Similar to what was observed for primary tumor growth, we did not detect statistical differences in metastatic capacity between siNEG and siAT-treated mice (Fig. 4). In conclusion, induction of a hypercoagulable state with associate thrombosis in tumor bearing mice, at least in our spontaneous model, does not lead to enhanced tumor progression. Nevertheless, our study is subject to a number of limitations. First of all, we made use of a low AT model that induces a systemic hypercoagulable state, rather than the formation of a localized thrombus in e.g. the legs. It is important to mention that in previous studies low AT induced a spontaneous hypercoagulable phenotype when combined with low protein C, [18] presence of Factor V Leiden 'knock-in' alleles (unpublished data), or severe hypercholesterolemia due to apolipoprotein E deficiency [20]. In the siAT/siPC hypercoagulant model TF, thrombin, and platelets are essential to the formation of thrombi, however FXII and neutrophils, considered key players in thrombosis as determined in other VTE models such as the stenosis and electrolytic VTE model [21] do not play a role in the siAT/siPC-dependent hypercoagulant phenotype [22]. In line with these results, it is likely that FXII and neutrophils are likewise not keyplayers in the siAT hypercoagulant model, which is a limitation in the model used. Both neutrophils and FXII also play important roles in (vascular) inflammation [23], thus, in contrast to other venous thrombosis mouse models, inflammation may not be prominent in the siAT-dependent model. It is known that inflammation impacts cancer progression [24] and the absence of such an inflammatory state in our siAT model may have reduced the potential of tumor cells to metastasize.

We also point out that in our model, lowering AT levels were sufficient to induce this hypercoagulable state, in contrast to our previous studies, showing that simultaneous knockdown of protein C was required for this phenotype [18]. We hypothesize that the presence of a procoagulant tumor abrogates the necessity of this protein C knock down.

Second, we made use of an orthotopic breast cancer model. Earlier stages of breast cancer are not associated with dramatically increased risks of developing VTE, however VTE rate increases with enhanced progression [11]. The tumor cells used in this model are highly aggressive, prone to metastasis, and highly procoagulant. Nevertheless, future studies using this model may be considered using tumor cells that represent cancer types associated with a higher risk of VTE, such as pancreatic cancer or glioblastoma.

Thirdly, we have used immune-compromised Nod-SCID mice, allowing us to study human cancer cells in a mouse model. The Nod-SCID mice used lack B and T cells, but NK cells can still be activated [25]. In line, Dewan and coworkers demonstrated that Nod-SCID mice treated with a TMβ1 antibody, transiently abrogating NK cell activity, resulted in increased metastasis of s.c. injected MDA-MB-231 cells, demonstrating that NK cells in Nod-SCID mice are functionally active in targeting breast cancer cells [26]. A comparable role for B and T cells can be speculated upon, but has not been established.

Thus, in future experiments effects of venous thrombosis or hypercoagulation on tumor progression should be detailed in other murine venous thrombosis models incorporating more immune system parameters and using cancer types associated with a higher VTE risk such as colorectal cancer, lung cancer and pancreatic cancer [11].

Finally we wish to point out that while induction of a hypercoagulable state in our previous publications led to such a severe phenotype that animals needed to be sacrificed. In the current experiments, animals appeared to recover 7–10 days after siAT treatment, as evidenced by

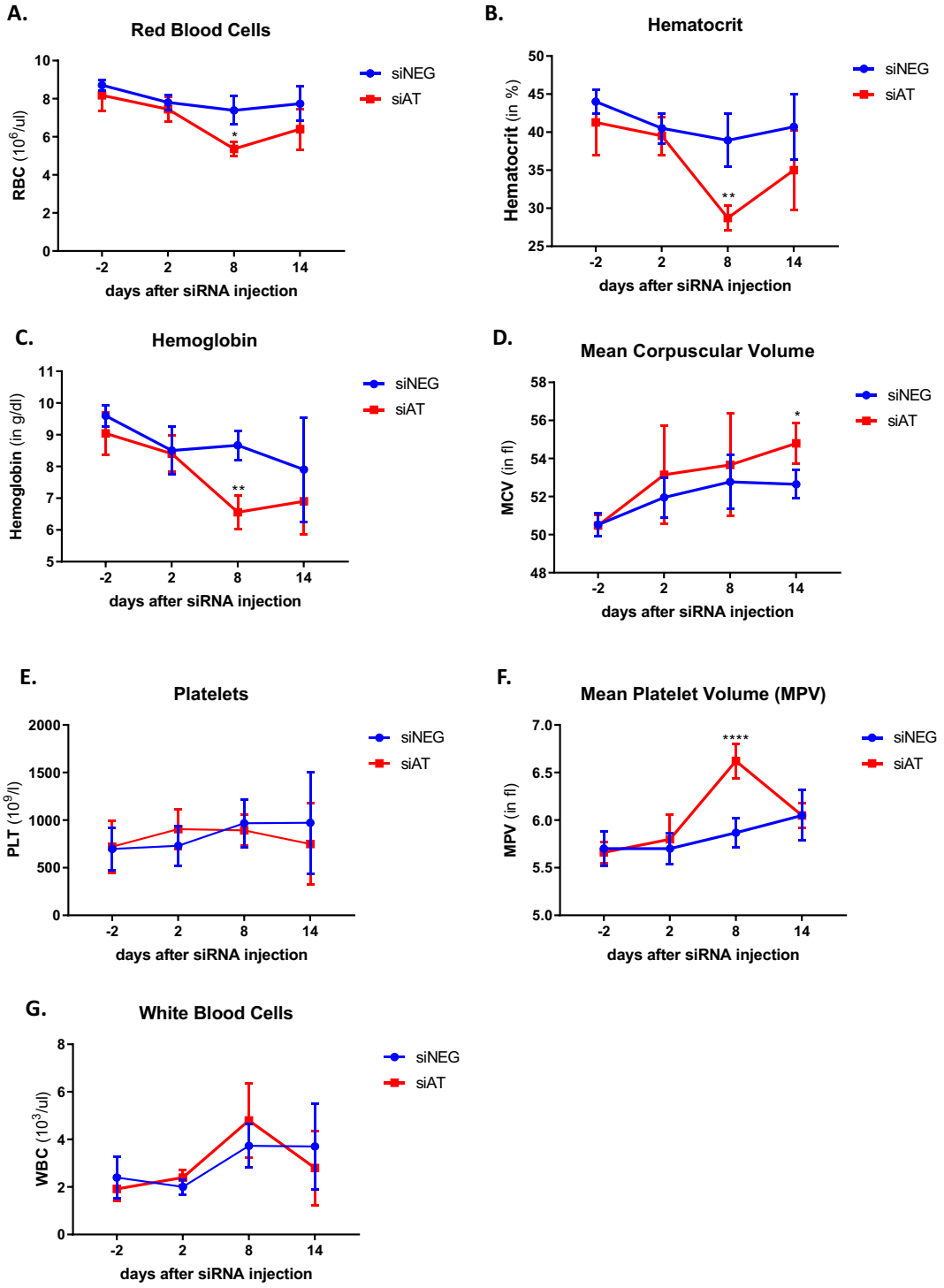

Fig. 2. Effects of systemic antithrombin knockdown on blood parameters. Citrated blood samples were taken and the following blood parameters were assessed on a hematology analyzer (Sysmex XP-300): red blood cells (A), hematocrit (B), hemoglobin (C), mean corpuscular volume (D), platelets (E), mean platelet volume (F) and white blood cells (G). Data (siAT: $n = 5$; siNEG: $n = 4$) are represented as mean with standard deviation; *P < 0.05, **P < 0.01, ***P < 0.001 using two-way ANOVA with Bonferroni post-hoc testing. (For interpretation of the references to colour in this figure legend, the reader is referred to the web version of this article.)

increasing body weight. One explanation for this may be the bolus injections of glucose. However, unpublished work indicates that the presence of a breast tumor may protect somewhat from the weight drop caused by siAT.

In conclusion, we show in a spontaneous mouse model that induction of hypercoagulation by knocking down AT does not per sé impact tumor growth or metastasis.

CRediT authorship contribution statement

J.T.B., B.U., B.v.V. and H.H.V. designed the study. H.H.V. acquired funding. J.T.B., B.U. M.H., E.H.L performed experiments. J.T.B. performed data analysis. J.T.B., B.U., B.v.V., H.H.V. were responsible for data interpretation. All authors critically reviewed the manuscript for intellectual content and approved the final version.

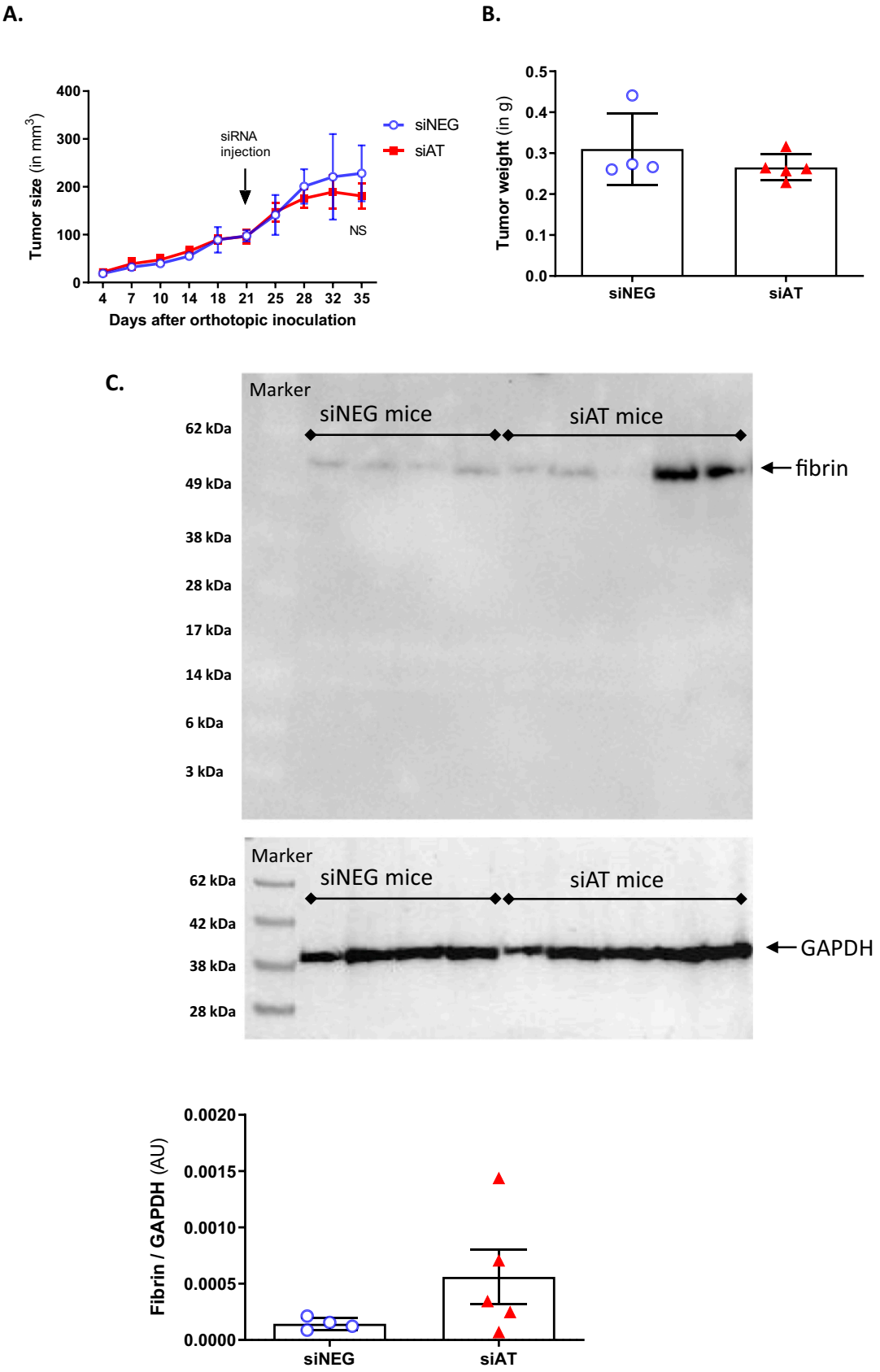

Fig. 3. Systemic knockdown of antithrombin does not affect MDA-MB-231 tumor growth at primary site in NOD-SCID mice. A. 1×10^6/50ul MDA-MB-231 cells were orthotopically inoculated into the 4th mammary fatpad of NOD-SCID mice, and measured twice a week using a caliper (A) and excised and weighed at the end of the experiment (B). Data (siAT: $n = 5$; siNEG: $n = 4$) are represented as mean with standard deviation. C. Western blot demonstrating fibrin deposition in the tumor using a fibrin monoclonal antibody as well as GAPDH levels as a loading control. D. Plot showing quantified bands of the western blot in C. Quantified fibrin levels were normalized for GAPDH signal.

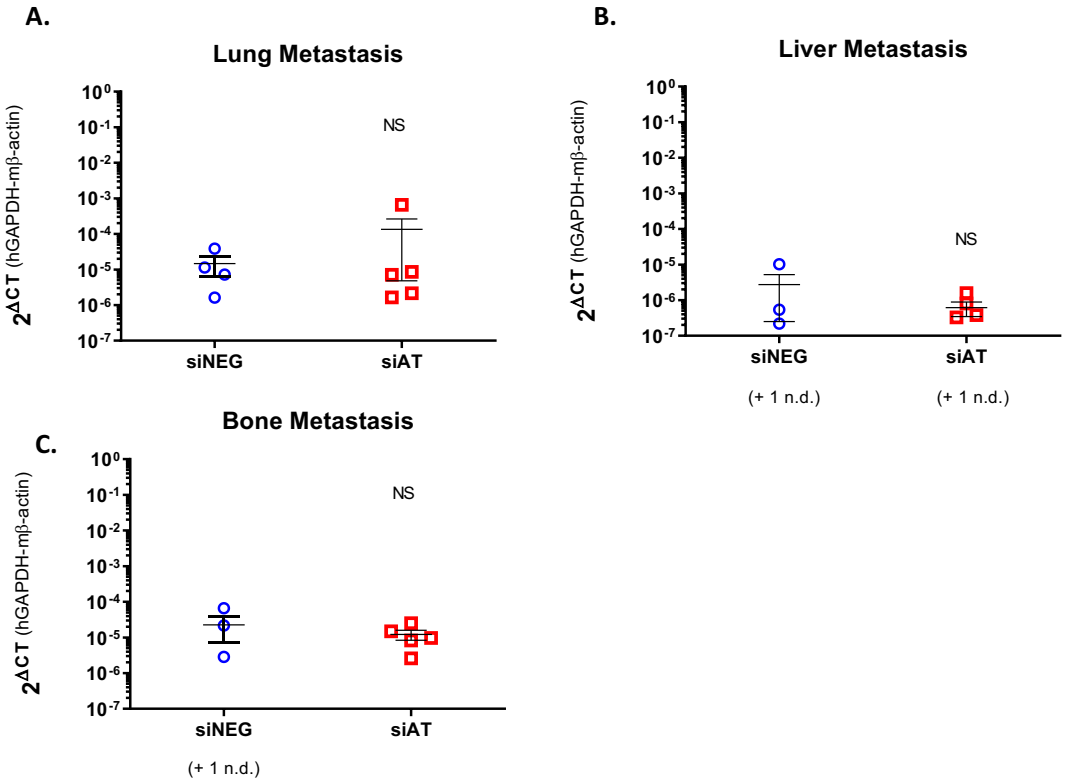

Fig. 4. Systemic knockdown of antithrombin does not affect MDA-MB-231 metastasis to distant organs in NOD-SCID mice. Quantitative RT-PCR (qPCR) using human specific primers to detect human MDA-MB-231 cancer cells in lung (A), liver (B) and bone marrow of the tibia (C). Data (siAT: n = 5; siNEG: n = 4) are represented as mean with standard deviation. In the liver of 1 siNEG and 1 siAT mouse, and in the bone marrow of 1 siNEG mouse no cancer cells were detected (n.d.).

Declaration of competing interest

The authors have nothing to disclose with regard to commercial support.

Data availability

Data are available upon request.

Acknowledgements

The authors gratefully acknowledge support from the Dutch Digestive Foundation (#SK 18-17) and Dutch Cancer Society (#13189). Finally, the authors acknowledge support from ZonMW, project number 114024066.

Appendix A. Supplementary data

Supplementary data to this article can be found online at https://doi.org/10.1016/j.thromres.2022.11.018.

References

[1] A.M. Gil-Bernabé, S. Lucotti, R.J. Muschel, Coagulation and metastasis: what does the experimental literature tell us? Br. J. Haematol. 162 (4) (2013 Aug) 433–441.
[2] H.H. Versteeg, J.W. Heemskerk, M. Levi, P.H. Reitsma, New fundamentals in hemostasis, Physiol. Rev. 93 (1) (2013 Jan) 327–358.
[3] Y.W. van den Berg, S. Osanto, P.H. Reitsma, H.H. Versteeg, The relationship between tissue factor and cancer progression: insights from bench and bedside, Blood 119 (4) (2012 Jan 26) 924–932.
[4] A.M.R. Rondon, C. Kroone, M.Y. Kapteijn, H.H. Versteeg, J.T. Buijs, Role of tissue factor in tumor progression and cancer-associated thrombosis, Semin. Thromb. Hemost. 45 (4) (2019 Jun) 396–412.
[5] M.Z. Wojtukiewicz, D. Hempel, E. Sierko, S.C. Tucker, K.V. Honn, Protease-activated receptors (PARs)–biology and role in cancer invasion and metastasis, Cancer Metastasis Rev. 34 (4) (2015 Dec) 775–796.
[6] J.S. Palumbo, K.E. Talmage, J.V. Massari, C.M. La Jeunesse, M.J. Flick, K. W. Kombrinck, Z. Hu, K.A. Barney, J.L. Degen, Tumor cell-associated tissue factor and circulating hemostatic factors cooperate to increase metastatic potential through natural killer cell-dependent and-independent mechanisms, Blood 110 (1) (2007 Jul 1) 133–141.
[7] D. Green, S. Karpatkin, Role of thrombin as a tumor growth factor, Cell Cycle 9 (4) (2010 Feb 15) 656–661.
[8] C.P. Klerk, S.M. Smorenburg, H.M. Otten, A.W. Lensing, M.H. Prins, F. Piovella, P. Prandoni, M.M. Bos, D.J. Richel, G. van Tienhoven, H.R. Büller, The effect of low molecular weight heparin on survival in patients with advanced malignancy, J. Clin. Oncol. 23 (10) (2005 Apr 1) 2130–2135.
[9] A.K. Kakkar, M.N. Levine, Z. Kadziola, N.R. Lemoine, V. Low, H.K. Patel, G. Rustin, M. Thomas, M. Quigley, R.C. Williamson, Low molecular weight heparin, therapy with dalteparin, and survival in advanced cancer: the fragmin advanced malignancy outcome study (FAMOUS), J. Clin. Oncol. (22) (2004) 1944–1948, thromboembolism. J Clin Oncol. 2005 Apr 1;23(10):2123-9.
[10] D. Sanford, A. Naidu, N. Alizadeh, A. Lazo-Langner, The effect of low molecular weight heparin on survival in cancer patients: an updated systematic review and meta-analysis of randomized trials, J. Thromb. Haemost. 12 (7) (2014 Jul) 1076–1085.
[11] J.F. Timp, S.K. Braekkan, H.H. Versteeg, S.C. Cannegieter, Epidemiology of cancer-associated venous thrombosis, Blood 122 (10) (2013 Sep 5) 1712–1723.
[12] F.I. Mulder, E. Horváth-Puhó, N. van Es, H.W.M. van Laarhoven, L. Pedersen, F. Moik, C. Ay, H.R. Büller, H.T. Sørensen, Venous thromboembolism in cancer patients: a population-based cohort study, Blood 137 (14) (2021 Apr 8) 1959–1969.
[13] B. Ünlü, N. van Es, W. Arindrarto, S.M. Kiełbasa, H. Mei, J. Westerga, S. Middeldorp, P.J.K. Kuppen, J.M.M.B. Otten, S. Cannegieter, H.H. Versteeg, Genes associated with venous thromboembolism in colorectal cancer patients, J. Thromb. Haemost. 16 (2) (2018 Feb) 293–302.
[14] J.T. Buijs, E.H. Laghmani, R.F.P. van den Akker, C. Tieken, E.M. Vletter, K.M. van der Molen, J.J. Crooijmans, C. Kroone, S.E. Le Dévédec, G. van der Pluijm, H. H. Versteeg, The direct oral anticoagulants rivaroxaban and dabigatran do not inhibit orthotopic growth and metastasis of human breast cancer in mice, J. Thromb. Haemost. 17 (6) (2019 Jun) 951–963.
[15] A.C. Cleuren, B. van Hoef, M.F. Hoylaerts, B.J. van Vlijmen, H.R. Lijnen, Short-term ethinyl estradiol treatment suppresses inferior caval vein thrombosis in obese mice, Thromb. Haemost. 102 (5) (2009 Nov) 993–1000.
[16] S.N. Tchaikovski, B.J. Van Vlijmen, J. Rosing, G. Tans, Development of a calibrated automated thrombography based thrombin generation test in mouse plasma, J. Thromb. Haemost. 5 (10) (2007 Oct) 2079–2086.
[17] J.T. Buijs, E.H. Laghmani, R.F.P. van den Akker, C. Tieken, E.M. Vletter, K.M. van der Molen, J.J. Crooijmans, C. Kroone, S.E. Le Dévédec, G. van der Pluijm, H.

H. Versteeg, The direct oral anticoagulants rivaroxaban and dabigatran do not inhibit orthotopic growth and metastasis of human breast cancer in mice, J. Thromb. Haemost. 17 (6) (2019 Jun) 951–963.
[18] H. Safdar, K.L. Cheung, D. Salvatori, H.H. Versteeg, H. Laghmani el, G. T. Wagenaar, P.H. Reitsma, B.J. van Vlijmen, Acute and severe coagulopathy in adult mice following silencing of hepatic antithrombin and protein C production, Blood 121 (21) (2013 May 23) 4413–4416.
[19] B. Kocatürk, H.H. Versteeg, Orthotopic injection of breast cancer cells into the mammary fat pad of mice to study tumor growth, J. Vis. Exp. 96 (2015 Feb 8) 51967.
[20] A.B. Ouweneel, M. Heestermans, R.A.F. Verwilligen, M.J.J. Gijbels, P.H. Reitsma, M. Van Eck, B.J.M. van Vlijmen, Silencing of anticoagulant protein C evokes low-incident but spontaneous atherothrombosis in apolipoprotein E-deficient mice-brief report, Arterioscler. Thromb. Vasc. Biol. 37 (5) (2017 May) 782–785.
[21] S.P. Grover, T.M. Olson, B.C. Cooley, N. Mackman, Model-dependent contributions of FXII and FXI to venous thrombosis in mice, J. Thromb. Haemost. 18 (11) (2020 Nov) 2899–2909.
[22] M. Heestermans, S. Salloum-Asfar, T. Streef, E.H. Laghmani, D. Salvatori, B. M. Luken, S.S. Zeerleder, H.M.H. Spronk, S.J. Korporaal, D. Kirchhofer, G.T. M. Wagenaar, H.H. Versteeg, P.H. Reitsma, T. Renné, B.J.M. van Vlijmen, Mouse venous thrombosis upon silencing of anticoagulants depends on tissue factor and platelets, not FXII or neutrophils, Blood 133 (19) (2019 May 9) 2090–2099.
[23] R.K. Mailer, C. Rangaswamy, S. Konrath, J. Emsley, T. Renné, An update on factor XII-driven vascular inflammation, Biochim. Biophys. Acta, Mol. Cell Res. 1869 (1) (2022 Jan), 119166.
[24] L.M. Coussens, Z. Werb, Inflammation and cancer, Nature 420 (6917) (2002 Dec 19–26) 860–867.
[25] M. Ito, H. Hiramatsu, K. Kobayashi, K. Suzue, M. Kawahata, K. Hioki, Y. Ueyama, Y. Koyanagi, K. Sugamura, K. Tsuji, T. Heike, T. Nakahata, NOD/SCID/gamma(c) (null) mouse: an excellent recipient mouse model for engraftment of human cells, Blood 100 (9) (2002 Nov 1) 3175–3182.
[26] M.Z. Dewan, H. Terunuma, M. Takada, Y. Tanaka, H. Abe, T. Sata, M. Toi, N. Yamamoto, Role of natural killer cells in hormone-independent rapid tumor formation and spontaneous metastasis of breast cancer cells in vivo, Breast Cancer Res. Treat. 104 (3) (2007 Sep) 267–275.